SHORTWAVE INFRARED IMAGING SPECTROSCOPY FOR ANALYSIS OF ANCIENT PAINTINGS

Taixia Wu[1] Guanghua Li[2] Zehua Yang[2] Hongming Zhang[1]. Yong Lei[2] Nan Wang[1] Lifu Zhang[1]
[1] Institute of Remote Sensing and Digital Earth, Chinese Academy of Sciences, Beijing 100101, China,
Email:zhanglf@radi.ac.cn
[2] The Palace Museum, Beijing 100009, China

KEY WORDS: Hyperspectral; shortwave infrared; imaging spectrometer; historic preservation; the ancient paintings.

ABSTRACT: Spectral analysis is one of the main non-destructive techniques used to examine cultural relics. Hyperspectral imaging technology, especially on the shortwave infrared band, can clearly extract information from paintings, such as color, pigment composition, damage characteristics, and painting techniques. All of these characteristics have significant scientific and practical value in the study of ancient paintings and other relics and in their protection and restoration. In this study, an ancient painting numbered Gu-6541, which had been found in the Forbidden City, served as a sample. A ground-based shortwave infrared imaging spectrometer was used to produce hyperspectral images with high spatial and spectral resolution. Results indicated that shortwave infrared imaging spectral data greatly facilitates the extraction of line features used in drafting, even using single band image. It can be used to identify and classify mineral pigments used in the painting. These images can detect alterations and traces of daub used in painting corrections and, combined with hyperspectral data analysis methods such as band combination or principal component analysis, such information can be extracted to highlight outcomes of interest. In brief, the SWIR imaging spectral technique was found to have a highly favorable effect on the extraction of line features from drawings and on the identification of colors, classification of paintings, and extraction of hidden information.

1. INTRODUCTION

In the long river of history, human beings have created many splendid artistic objects, and painting is an important form of artistic expression of Chinese civilization. Paintings number among the great treasures of Chinese art. The history of painting in China dates back to ancient times, through the late Qing Dynasty, covering a period of over four thousand years. Ancient painting includes everything from Neolithic pottery and prehistoric rock painting with patterns and decorations, painted bronzeware from the Shang and Zhou Dynasties, silk paintings from the Warring States period and Western Han Dynasty, original lacquer painting from the Qin Dynasty, Qin and Han Dynasty tomb murals, portraits on brick and woodcut from the Han Dynasty, and the famous silk and paper paintings that have been made by famous painters since the beginning of the Six Dynasties. These categories of paintings form the long and uninterrupted history of Chinese painting, and they have impressed many viewers with their profound brilliance[1].

The extraction of line information from ancient cultural relics, characterization of pigment composition, and search for hidden information are of great significance to the research, protection, and restoration of ancient paintings [2]. Currently, non-destructive testing for ancient paintings depends mainly on spectral analysis technology[3-5]. Multi-spectral and hyperspectral analysis technology can provide analysts with a deeper, clearer, and more intuitive understanding of the color, damage characteristics, pigment composition, and techniques used to make the painting [6-8].

For a long time, researches of multi/hyperspectral imaging focused on remote sensing field. In recent years, however, scholars have recognized the practical value of multi/hyperspectral imaging technology in the study of cultural relics, and a great deal of useful results have been reported [9, 10]. However the wavelengths used by multi/hyperspectral imaging techniques are mainly concentrated in the visible/near infrared band (400–1000 nm) [11-14], some researches noticed the important spectral characters at 1000-1700 nm[15, 16]. However, the use of longer wavelengths (especially 1700-2500 nm) has only rarely been reported.

Shortwave infrared (SWIR) is infrared with bands of 1000 to 2500 nm. SWIR reflected by materials have different SWIR reflection characteristics [17]. These provided direct and effective techniques for applications such as identifying the lines in drawings and the pigments in ancient paintings. The imaging spectrum data acquired by the shortwave infrared ground spectral imaging systems have high spatial resolution and high spectral resolution at the same time. This is conducive to finding objects on the Earth's surface using texture and spectral analysis, which is especially suitable in close-range photogrammetry[18]. In this study, an ancient Chinese painting was used as an example. It's imaging spectrum data were obtained at a wavelength of 1000–2500 nm using a ground-based shortwave infrared imaging spectrometer. The features of line sketches such as the original line draft can be extracted by certain single band image directly, without any data processing work. Using hyperspectral image processing techniques, such as band combination, image enhancement, and transformation, certain pigment colors and hidden information can be enhanced for effective extraction. The shortwave infrared imaging spectrometer may play an important role in the

production of digital archives and in the analysis and restoration of cultural relics and so promote the development of digital work associated with cultural relics.

2. METHODS AND MATERIALS

2.1 Ancient painting samples

The ancient painting that served as in the present study is currently stored in the Forbidden City and numbered Gu-6541. When it was first discovered, it was called "Wanshou painting for Yongyan (seventh emperor of the Qing Dynasty) by an artist from the Qing Dynasty." Shu Lin from the Palace Museum compared the image to historical archives from the Qianlong period and concluded that this image was painted for the 80th birthday of the Empress Dowager Chongqing by an artist named Wenhan Yao. The painting is 219 cm long and 285 cm wide, painted on colored silk. The picture was mounted on four sides with blue damask silk using a method called Tieluo. The frame is 232.5 long and 286.5 cm wide. The image in the picture can be considered in two parts. The first part depicts seven main halls facing south, and covered with glazed tiles. The main figure is an elderly woman wearing Qing Dynasty robes, a phoenix coronet, and earrings decorated with golden dragons holding beads in their mouths. The woman sits up straight on the throne in front of a folding screen. The second part is a carving painted to show a yellow cloth pavilion in the middle. A long table with tuoni, a traditional decoration, is set in the pavilion. There is also "zun" (drinking cups), golden lei (ancient urn-shaped vessels), golden zhi (ancient wine vessels), and golden jue (drinking vessels) and goblets for serving wine. Several realistic figures are present in the picture, providing abundant content. The realistic drawing style establishes that this is a documentary painting, and its historical value is significantly greater than its artistic value[19].

Fig. 1 Ancient painting of Qing Dynasty stored in the Forbidden City (No. Gu-6541)

2.2 Shortwave infrared imaging spectrometer and data acquisition

A ground-based shortwave infrared imaging spectrometer was used as measuring instrument in this research. The right panel of Fig. 2(a) shows the physical picture for shortwave infrared imaging spectrometer system. The middle row of images, from right to left, show a scanning mirror, infrared imaging lens, spectral light splitter, and HgCdTe infrared detector[20]. The detector with 320*256 pixels. The swing scanning mirror is driven by the electric motor, and it sweeps back and forth to spectrally image the sample in the field of view. Infrared imaging uses lenses in the shortwave infrared range, which match the spectral range of optical splitters and detector. The optical splitter is a shortwave infrared PGP manufactured by Finland Specim Company with a spectral range from 1000–2500 nm and slit width of 30 nm. The spectral resolution of the splitter is about 10 nm. The field of view is less than 2.0 mrad. Because shortwave infrared imaging is very sensitive to changes in temperature, the panel detector uses four-grade semiconductor refrigeration to cool the photosensitive surface of the detector. Temperatures 80° below ambient can be reached. An iron loop was fixed to the external side of PGP splitter component and its top was connected to the photography tripod, which was used to fix the overall system.

Fig. 2(b) shows the principle underlying the use of shortwave infrared imaging spectrometer system in the ground. The reflection light signal of each ground object entered the objective lens through the reflection from the front mirror, and the light was collected and focused on the slit on the front end of the PGP splitter. Optical signals other than those

from the ground sample were blocked by the slit and spectral resolution was determined collectively by the slit and by the components of the splitter and detector. The light passing through the slit was collimated by the lens in the PGP splitter and the incident light was directed to the prism grating prism light splitter. After dispersion, light of different wavelengths was distributed to different physical locations. With the convergence of focusing lens in the PGP optical device, an image forms on the photosensitive surface of the detector array, and spatial dimension information of ground objects can be determined parallel to the direction of the slit, and spectral dimension information of the ground objects can be found vertical to the direction of the slit. The spectral data acquired by the surface array detector is transmitted to the notebook computer for processing, display and storage. The SWIR data achieved with this system provided "image-spectrum combined" information. Ground measurement not only provided high-resolution images of the object but also the spectral curve of each pixel in the image. This method increases the work efficiency of field surface spectrum measurement and provides abundant data information for spectral analysis, spectral decomposition, and the extraction of pure pixels[21, 22].

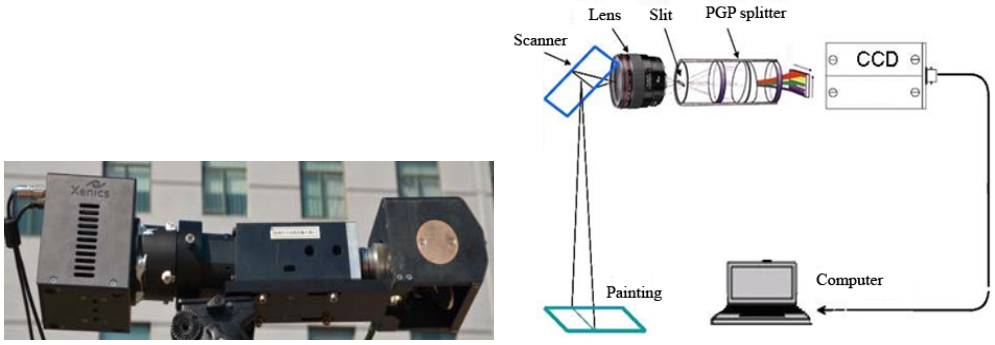

(a) (b)

Fig. 2 Physical and schematic diagram of the shortwave infrared imaging spectrometer system

The data acquisition process is described briefly as follows: The painting was hung on the wall and a halogen lamp served as a light source. The shortwave infrared imaging spectrometer was placed parallel to the picture during the scan. A standard diffuse reflection plate served as standard during the experiment to calculate reflectance. The data acquisition is based on self-developed data acquisition program.

2.3 Data analysis method

(1) Reflectance correction

The scanned hyperspectral imaging data is raw digital number (DN) image and can be transferred as radiance image. Radiance cannot be used directly for spectral analysis because illumination depends on date and meteorological conditions. It first needs reflectance correction.

For Lambertian surfaces, as a first approximation, radiance $L(\lambda)$ is the product of the target reflectance $R(\lambda)$, which is intrinsic information and the illumination during image acquisition, i.e. in this case halogen lamp lighting $E(\lambda)$.

$$L(\lambda) = R(\lambda) \cdot E(\lambda) \tag{1}$$

To solve for the variable of interest reflectance R, it is necessary to know the illumination. For that purpose, a calibrated Lambertian diffuser whiteboard was placed in the field of view of the imaging spectrometer. In given lighting conditions, the following is true:

$$L_{\text{target}} = R_{\text{target}} \cdot E \tag{2}$$

$$L_{\text{ref}} = R_{\text{ref}} \cdot E \tag{3}$$

$$R_{\text{target}} = \frac{L_{\text{target}}}{L_{\text{ref}}} \cdot R_{\text{ref}} \tag{4}$$

Here, R designates the reflectance, L the radiance, and ref the reference[23].

(2) Spectral angle mapper classification algorithm

Supervised classification is a technique based on statistical identification, and based on typical sample training method for classification. Spectra angle mapper (SAM), an algorithm based on the overall similarity of the spectral curve, is often used in high spectral data processing. SAM calculates the angle between the test spectra and reference

spectrum to describe the similarity between the two. Small angles between the two spectra indicate high similarity[24]. The length of a ($L\rho$) is calculated as follows:

$$L_\rho = \sqrt{\sum_{\lambda=1}^{M} \rho_\lambda^2} \tag{5}$$

The spectral angle (θ) is calculated as follows:

$$\theta = \cos^{-1}\left(\frac{\sum_{\lambda=1}^{M} \rho_\lambda \rho'_\lambda}{L_\rho L_{\rho'}} \right) \tag{6}$$

Here, L_ρ and $L_{\rho'}$ is the length of the test spectrum and reference spectrum vector respectively. θ is the angle between the test spectrum and reference spectrum. The range of values for θ was [0, π/2], with smaller values indicating greater similarity between the test and reference spectra, which in turn indicated a higher probability and more accurate classification. The size of the spectral angle, regardless of the radiance, was related only to the vector directions of the two spectra to be compared, which diminished the effect of illuminance and landscape on the measurement of similarity.

(3) Principal component analysis

Principal component analysis (PCA) can be used to reduce the dimensionality of a hyperspectral imaging data without losing significant amount of information. This can be considered a data compression technique that puts redundant or correlated information into separate variables. It renders the transformed vectors orthogonal and uncorrelated thus removing any co-linearity problems[25].

PCA is a linear transformation that projects data onto a new orthogonal feature space in a way that the first few components in the new feature space will represent most of the variances in the original dataset. The transformation is based on the second order statistics (covariance) of the original data. Assume x represents the vector of a pixel's grey value in an image of N bands. The transformation is defined as follows:

$$y = \mathbf{A}^t \cdot x \tag{7}$$

Here, **A** is the matrix of normalized eigenvectors of the image covariance matrix, and t denotes the transpose operation of the matrix. The image covariance matrix, **C**, is an N-by-N matrix and can be constructed according to all pixels, x_i , i = 1, 2, …, K and the mean vector m, as described in equation (8) and equation (9).

$$\mathbf{C} = E\left\{(x_i - m)(x_i - m)^t\right\} = (K-1)^{-1}\sum_{i=1}^{K}(x_i - m)(x_i - m)^t \tag{8}$$

$$m = E\{x\} = \frac{1}{K}\sum_{i=1}^{K} x_i \tag{9}$$

There are two tasks in a PCA. The first is an eigen analysis to generate the transformation matrix, A; and the second is the linear transformation for each pixel to project data onto the new orthogonal space y [26].

3. RESULTS AND ANALYSIS

3.1 Extraction of line drawing

Line drawing is the main technique used to design paintings. It forms the foundation of traditional Chinese traditional painting. Line drawing is not only an essential step in the overall drawing process but also contributes to picture composition, figure scale, light sources, and spatial relationships. Line drawing is also an important way to study the ancient painting style and painting process and prepare for protection and restoration. It is an important measure of China's Dunhuang mural protection and restoration. However because colored paint is added on top of most line drawings, distinguishing and extracting lines from drawings can be very difficult. The traditional line description system depends on manual operation, which despite its maturity, is a time-consuming and laborious process.

Fig. 3 Shortwave infrared imaging data at different wavelengths (longer wavelengths show more prominent line drafting)

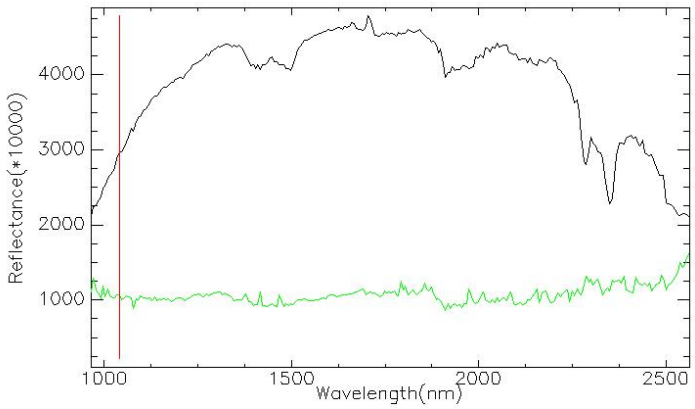

Fig.4 Shortwave infrared spectrum curves of clothes and carbon black pigment

Fig.5 Density slice for line drafting at 1804 nm

Fig. 3 shows the spectral data of shortwave infrared imaging with wavelengths ranging from 1000–2500 nm. A total of 8 images were extracted, each one at intervals of about 200 nm. Fig. 4 gives the spectral curves for clothes and carbon black pigment extracted from shortwave infrared imaging spectral data, with the longitudinal coordinates representing the reflectance and the transverse coordinates the band. The wavelength ranged from 1000–2500 nm. The upper curve in the figure shows the spectral curve of the dark blue pigment of clothes worn by figures in the painting, and the lower curve shows the spectral curve of black pigment used for outlining those clothes.

Each band image in Fig.3 shows that as wavelength increased, the color of the figure's clothes transitioned from dark to light, which is consistent with the spectral curve shown in Fig. 4. The spectral curve of pigment used for clothes showed increased reflectance from 1000 to 1400 nm, which means that the effect of the line drawing of the clothes and pigment differed across different bands. Little change of clothes color at wavelengths of 1600–2400 nm in Fig. 3, but differences in expression did show the man's chest pattern, the top of his hat, and the lower edge of the stool.

Unlike the pigment used for clothes, the black color used to outline the clothes produced a low value for all tested wavelengths and did not show any significant variation. As indicated with the lower curve in Fig. 4, black was shown in all images achieved with different wavelengths. Usually line sketches are drawn with pigments such as carbon black, which shows strong absorption along all wavelengths in shortwave infrared, contrasted with the pigments with relatively high reflection that resulted with light color in images produced with tested wavelengths, providing contrast marked enough to extract lines drawn with carbon black. This also explains the physical basis of shortwave infrared data extraction for line drafting. Fig. 5 is the line drafting extraction results, which shows a shortwave infrared image at 1804 nm band and colored the relatively low values pixels with blue using density slice method[27]. Density slicing is done by dividing the range of brightnesses in a single band into intervals, then assigning each interval to a color. It shows the shortwave infrared imaging spectral data provided a satisfactory outcome for the extraction of line drafting.

3.2 Pigment information extraction

Pigment is the main component of the painting. Many of the enduring colors used in traditional Chinese painting can last long into modern times, and most of have principally mineral ingredients [28]. For comparison, a portable ground object spectrometer (Model PSR-3500) manufactured by the American Spectral Evolution company was used in the study to test the spectrum ranged 400–2500 nm for multiple pigments. The shortwave infrared spectrum (1000-2500nm) of 12 kinds of typical Chinese painting pigments curves are shown in Fig. 6. The pigments are cadmium yellow, clam powder, white lead, red lead, ultramarine, mineral green, azurite, khaki, realgar, iron oxide, ocher and cinnabar. Azurite, also known as blue copper ore, is an alkaline copper carbonate mineral with the chemical formula $2CuCO_3 \cdot Cu(OH)_2$. The absorption valleys were detected at 1495 nm, 2282 nm, and 2351 nm. The main cause of the formation of the three spectral absorption features is the strong absorption of hydroxyl and carbonate in corresponding position, among which the latter two are more characteristic and more helpful in identifying azurite. Compare the spectral curve of pigment used for clothes in Fig. 4 to Fig. 6, it is clearly that the clothes pigment spectral absorption positions in Fig. 4 are agreed with azurite completely. Then the pigment used for clothes in Fig. 4 can be identified as azurite.

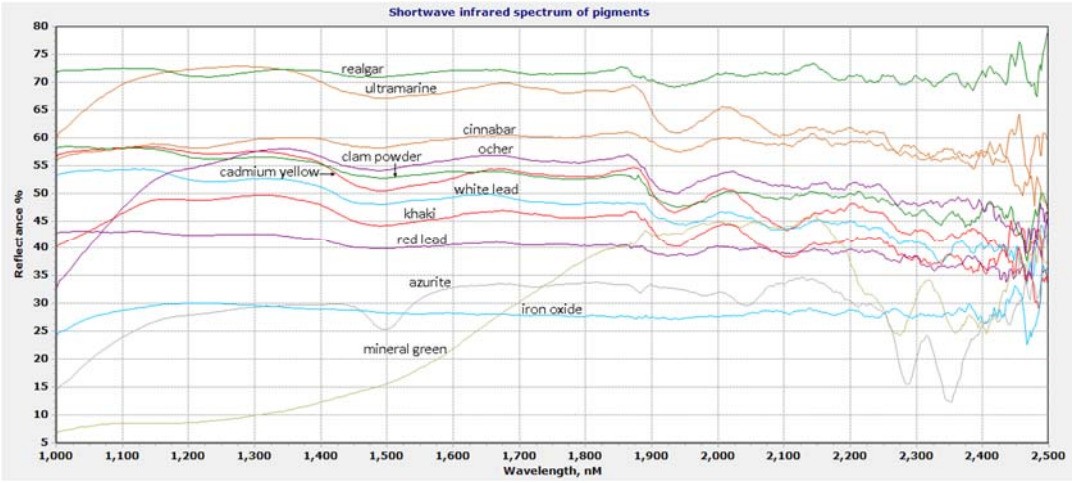

Fig. 6 Shortwave infrared spectrum of main Chinese painting pigments (by PSR-3500)

Based on the pigment determination made in Fig. 6, batch extraction was performed for pigments used in the ancient painting using SAM and supervised classification.

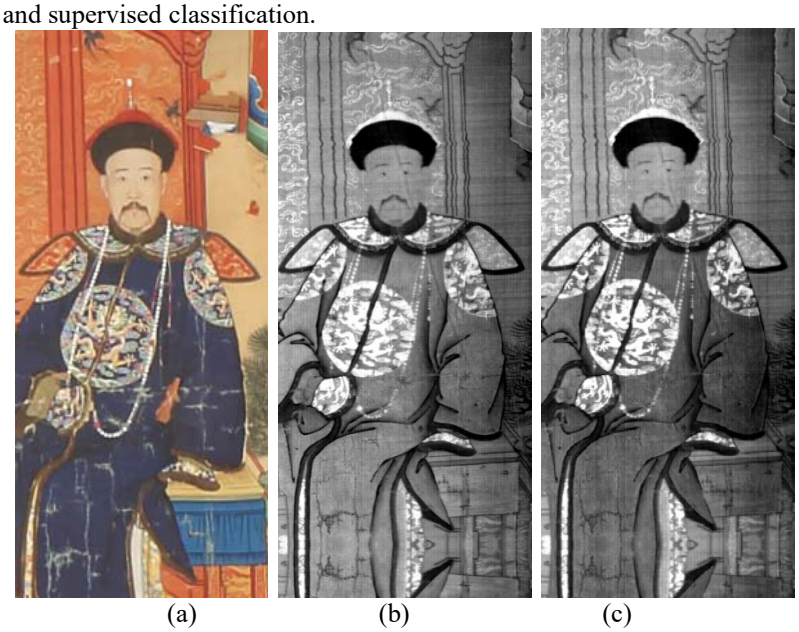

(a) (b) (c)

(d) (e) (f)

Fig.7 Extraction of spectral angle mapper for pigment used for clothes and background. (a) RGB image. (b, c) Images produced with wavelengths of 2282 nm and 2351 nm, respectively. (d) Azurite extraction of clothes with SAM technique. (e) False color composition image with result (d) and 1159 nm image. (f) Background spectral extraction.

Fig. 7(a) shows an RGB image. Fig. 7(b, c) shows images at 2282 nm and 2351 nm, respectively, and Fig. 7(d) shows the results of extracting azurite used in clothes using SAM. It have rather good extractions of the dark blue part of the sample picture, the bottom of the stool, and part of the ribbon on the upper right corner, all of these areas were painted by azurite. The Fig. 7(d) image was combined with the 1159 nm wavelength of original hyperspectral image for false color composition[29], shown in Fig. 7(e), which simulated the effects of putting clothes on the figure in the picture. The background of the picture, which was yellow, was similarly extracted using SAM, and results showed the wall and faces of the figures to have been colored with same pigment.

The curves showed in Fig. 6 mainly are spectrum of mineral pigments. One big advantage of the mineral pigments be chosen for painting is that it have stable physicochemical property and not easy to fade. The different of mineral spectral respective contributions of its cation and anionic groups to optical response. Not only the azurite can extracted using the shortwave infrared imaging spectral data as shown in Fig. 7, but also many other mineral pigments can be identified from it. Have a look at Fig. 6, the spectral features are more complicated and identifiable at 2200-2500 nm than 1000-2200 nm. The spectral band of 2200-2500 nm are mainly identification band of anionic groups. Take the malachite[30] (mineral green, chemical formula $CuCO_3 \cdot Cu(OH)_2$) for example, it presents an atypical carbonate ion spectrum, like azurite. The absorption valleys are shown at 2270 nm, 2362 nm, and 2406 nm. Using these spectral features, the malachite pigment can also be extracted from the shortwave infrared imaging spectral data, as shown in Fig. 8. The green color shown in Fig. 8 (left) are all malachite pigment and it can be classified well, as blue color parts in Fig. 8 (right). From Fig. 7 and Fig. 8, it show clearly the “image-spectrum combined” SWIR imaging spectral data have the ability to recognize and classify mineral pigments of painting. The spectrum information can recognize the pigments while the image show the pigments spatial distribution on the painting.

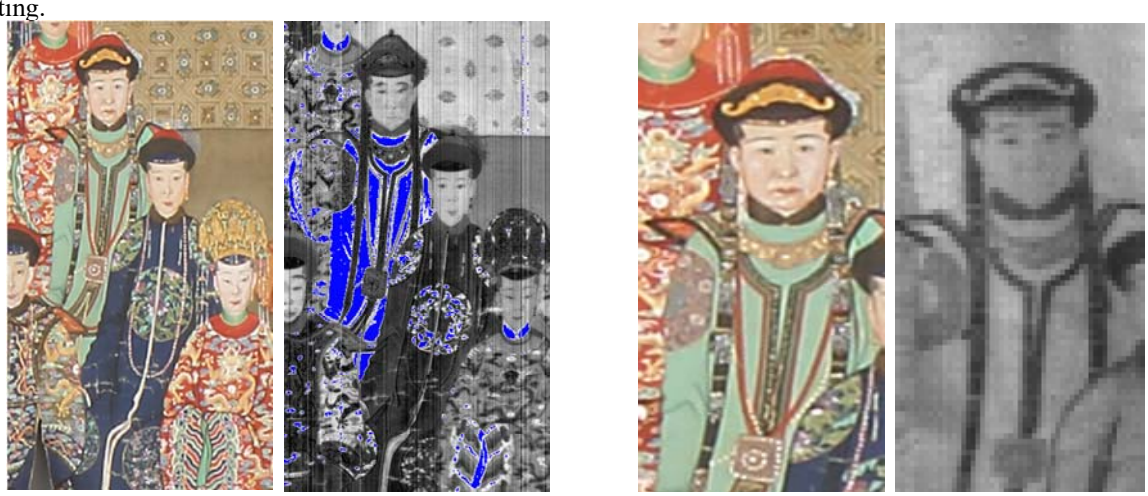

Fig.8 Mineral green pigment extraction from the shortwave infrared imaging spectral data. (The left is RGB image, and the blue parts in right is malachite pigment identification result)

Fig.9 Illegible information of the braid from the image detected at 1547 nm. The left is RGB image, and the right is 1574 nm image, the braid highly visible at the right image.

3.3 Extraction of hidden information

The hidden information in paintings generally includes signs of repair, hidden text patterns, and illegible information. Fig. 9 is intercepted part from the painting, in which certain patterns and decorations are visible in the woman's braids. The pattern was not significantly visible in the original RGB image, but extremely outstanding when detected with SWIR at wavelength of 1547 nm. This indicated that some information not readily visible under visible light can be identified and extracted effectively using shortwave infrared data.

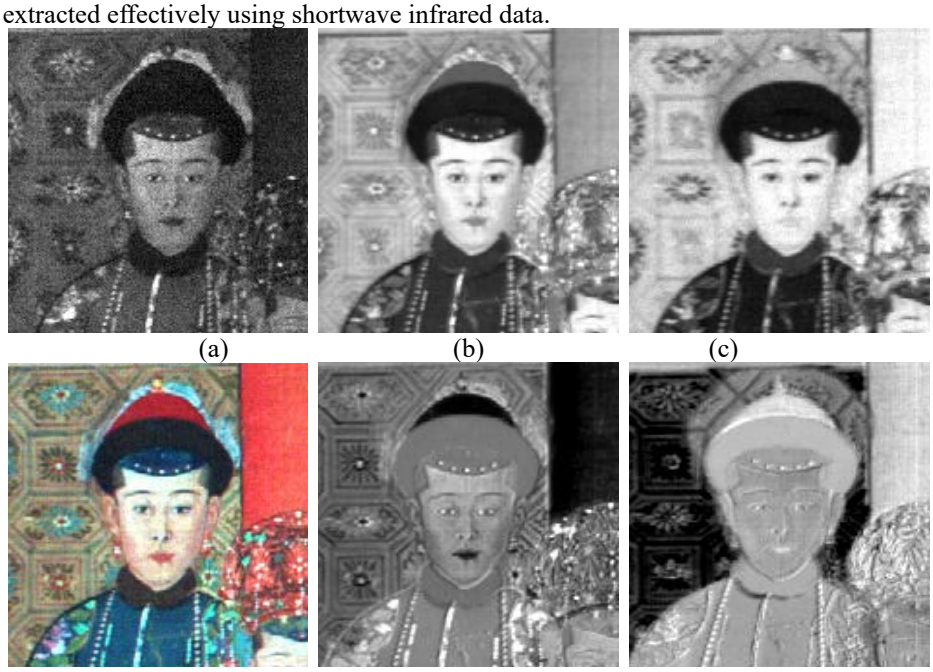

Fig. 10 Extraction of traces of corrections. (a) 453 nm image, (b) 980 nm image, (c) 1302 nm image, (d) false color composition image corresponding to images at 690 nm, 514 nm, and 453 nm, with significantly visible correction marks, (e) PCA2 image, (f) PCA3 image. (e) and (f) are images of second and third principle components, which show different signs indicating corrections.

Fig. 10 shows the extraction of repaired correction marks. Fig. 10(a–c) corresponds to images produced at wavelengths of 453 nm, 980 nm, and 1302 nm, respectively. Results showed a trace of correction above the hat worn by the figure, with different traces displayed under different wavelengths. Most significant traces were observed with 453 nm, and the traces faded at 980 nm with color becoming darker in the upper half of the hat. The color of upper half of a hat was almost the same as the background at 1302 nm, but relatively large, semi-circular smear marks were detected at 1302 nm. Fig. 10(d) shows false color synthesis at 690 nm, 514 nm, and 453 nm, all of which highlighted the trace of corrections.

Fig. 10(e) and (f) are images of the second and third main components achieved from hyperspectral image using principal component analysis (PCA). Because there is high correlation between hyperspectral images detected with different wavelengths and because the images looked similar visually, some of the data were considered redundant and repetitive from the point of view of extracting useful information. The goal of PCA is to concentrate useful information in original images. This is achieved using multiple wavelengths on new images of principle components. The number of principle images should be as small as possible and the principal component images should not be related to each other, which means that information from each principal component does not overlap, thus greatly reducing the total amount of data and enhancing the image information [15]. The second principle component (PCA2) emphasized the traces of correction shown in Fig. 10(d). The third principle component (PCA3) showed a large, semi-circular pattern over the hat worn by the figure, which may be used to highlight the correction trace shown in Fig. 10(c).

Fig. 11 Information features of the third principle component. (The left is RGB image, and the right is the third principle component with emphasized pattern information.)

Characteristic information can also be highlighted by treating other parts of the ancient painting with PCA. As shown in Fig. 11, the false color composition image for PCA3 can highlight the figure's chest, the dragon pattern on the figure's arm, and the decorative pattern on the wall, which is useful for extraction of corresponding features and information. Summarized from the samples, SWIR imaging spectral data can easily identify the illegible information, reveal painting modification traces and enhance the detail information of paintings.

4. CONCLUSION

In this study, a ground-based shortwave infrared imaging spectrometer was used to perform hyperspectral imaging on an ancient painting in order to collect shortwave infrared spectral imaging data with high spatial resolution and high spectral resolution. The outcomes of the study can be summarized as follows: (1) Imaging spectrum data collected using ground-based shortwave infrared imaging spectrometer greatly facilitate the extraction of features of line drafting, and effective extraction can be performed directly using certain single band. (2) Shortwave infrared imaging spectrum data can be used to identify and classify mineral pigments. (3) Shortwave infrared imaging spectrum data can detect the trace of correction and, using techniques such as band combination and principal component analysis, such information can be extracted to highlight outcomes of interest.
The present research will expand the range of application of shortwave infrared imaging spectrum technology in the study of cultural relics, including digital archiving, heritage diagnosis, and repair and promote the development of the science and technology of examining cultural heritage.

References

1. Shan G. Chinese painting appreciation dictionary. Shanghai: Shanghai Lexicographical Publishing House, 2008.
2. Wu F, Yang W and Li D. Research on Art Painting Pigment Composition Recognition Based on Spectra Feature Fitting. Chinese Journal of Light Scattering. 2014; 26: 88-92.
3. Daffara C, Pampaloni E, Pezzati L, Barucci M and Fontana R. Scanning multispectral IR reflectography SMIRR: an advanced tool for art diagnostics. Accounts of chemical research. 2010; 43: 847-56.
4. Delaney JK, Ricciardi P, Glinsman LD, et al. Use of imaging spectroscopy, fiber optic reflectance spectroscopy, and X-ray fluorescence to map and identify pigments in illuminated manuscripts. Studies in Conservation. 2014; 59: 91-101.
5. Casini A, Lotti F, Picollo M, Stefani L and Buzzegoli E. Image spectroscopy mapping technique for noninvasive analysis of paintings. Studies in conservation. 1999; 44: 39-48.
6. Carcagni P, Della Patria A, Fontana R, et al. Multispectral imaging of paintings by optical scanning. Optics and Lasers in Engineering. 2007; 45: 360-7.
7. Fischer C and Kakoulli I. Multispectral and hyperspectral imaging technologies in conservation: current research and potential applications. Studies in Conservation. 2006; 51: 3-16.
8. Delaney JK, Walmsley E, Berrie BH and Fletcher CF. Multispectral imaging of paintings in the infrared to detect and map blue pigments. Proceedings of the National Academy of sciences. 2005: 120.
9. Cheng J-H and Sun D-W. Rapid and non-invasive detection of fish microbial spoilage by visible and near infrared hyperspectral imaging and multivariate analysis. LWT-Food Science and Technology. 2015; 62: 1060-8.

10. Kubik M. Hyperspectral imaging: a new technique for the non-invasive study of artworks. Physical techniques in the study of art, archaeology and cultural heritage. 2007; 2: 199-259.
11. Gong M-t and Feng P-l. Preliminary study on the application of hyperspectral imaging on the classification of and identification Chinese traditional pigments classification–a case study of spectral angle mapper. Sciences of Conservation and Archaeology. 2014; 26: 76-83.
12. Legrand S, Vanmeert F, Van der Snickt G, et al. Examination of historical paintings by state-of-the-art hyperspectral imaging methods: from scanning infra-red spectroscopy to computed X-ray laminography. Heritage Science. 2014; 2: 13.
13. Gu A and Shen W. Nondestructive identification of Chinese seal-ink on paintings based on near-infrared spectroscopy and chemometric. Sciences of Conservation and Archaeology. 2013; 25: 59-64.
14. Balas C, Papadakis V, Papadakis N, Papadakis A, Vazgiouraki E and Themelis G. A novel hyper-spectral imaging apparatus for the non-destructive analysis of objects of artistic and historic value. Journal of Cultural Heritage. 2003; 4: 330-7.
15. Delaney JK, Zeibel JG, Thoury M, et al. Visible and infrared imaging spectroscopy of Picasso's Harlequin Musician: mapping and identification of artist materials in situ. Appl Spectrosc. 2010; 64: 584-94.
16. Delaney JK, Thoury M, Zeibel JG, Ricciardi P, Morales KM and Dooley KA. Visible and infrared imaging spectroscopy of paintings and improved reflectography. Heritage Science. 2016; 4: 1-10.
17. Thompson AJ, Hauff PL and Robitaille AJ. Alteration mapping in exploration: application of short-wave infrared (SWIR) spectroscopy. SEG newsletter. 1999; 39: 16-27.
18. Zhang L, Huang C, Wu T, Zhang F and Tong Q. Laboratory calibration of a field imaging spectrometer system. Sensors. 2011; 11: 2408-25.
19. Lin S. The New Discovery of Empress Dowager Chóngqìng's 80th Birthday Celebration Painted by Yao Wenhan (in Chinese). Palace Museum Journal. 2015; 180: 54-66.
20. Shaban A. Determination of concrete properties using hyperspectral imaging technology: a review. Science Journal of Physics. 2013; 2013.
21. Wu T, Zhang L, Cen Y, Wang J and Tong Q. Light weight airborne imaging spectrometer remote sensing system for mineral exploration in China. SPIE Sensing Technology+ Applications. International Society for Optics and Photonics, 2014, p. 910406--8.
22. Zhang L, Sun X, Wu T and Zhang H. An Analysis of Shadow Effects on Spectral Vegetation Indexes Using a Ground-Based Imaging Spectrometer. Geoscience and Remote Sensing Letters, IEEE. 2015; 12: 2188-92.
23. Barnes R, Dhanoa M and Lister SJ. Standard normal variate transformation and de-trending of near-infrared diffuse reflectance spectra. Appl Spectrosc. 1989; 43: 772-7.
24. Yuhas RH, Goetz AF and Boardman JW. Discrimination among semi-arid landscape endmembers using the spectral angle mapper (SAM) algorithm. 1992.
25. Baronti S, Casini A, Lotti F and Porcinai S. Multispectral imaging system for the mapping of pigments in works of art by use of principal-component analysis. Applied optics. 1998; 37: 1299-309.
26. Jolliffe I. Principal component analysis. Wiley Online Library, 2002.
27. Knight A, Tindall D and Wilson B. A multitemporal multiple density slice method for wetland mapping across the state of Queensland, Australia. International Journal of Remote Sensing. 2009; 30: 3365-92.
28. Dooley KA, Conover DM, Glinsman LD and Delaney JK. Complementary standoff chemical imaging to map and identify artist materials in an early Italian Renaissance panel painting. Angewandte Chemie. 2014; 126: 13995-9.
29. Hayem-Ghez A, Ravaud E, Boust C, Bastian G, Menu M and Brodie-Linder N. Characterizing pigments with hyperspectral imaging variable false-color composites. Applied Physics A. 2015; 121: 939-47.
30. Hunt GR and Salisbury JW. Visible and near infrared spectra of minerals and rocks. II. Carbonates. Modern Geology. 1971; 2: 23-30.